Journal of Alloys and Compounds 509 (2011) 7152–7161

Contents lists available at ScienceDirect

Journal of Alloys and Compounds

journal homepage: www.elsevier.com/locate/jallcom

Interfacial microstructure and properties of Sn–0.7Cu–0.05Ni/Cu solder joint with rare earth Nd addition

Guang Zeng [a], Songbai Xue [a,*], Lili Gao [a], Liang Zhang [a], Yuhua Hu [a], Zhongmin Lai [b]

[a] College of Materials Science and Technology, Nanjing University of Aeronautics and Astronautics, No. 29 Yudao Street, Nanjing 210016, Jiangsu Province, People's Republic of China
[b] Provincial Key Lab of Advanced Welding Technology, Jiangsu University of Science and Technology, Zhenjiang 212003, People's Republic of China

ARTICLE INFO

Article history:
Received 6 January 2011
Received in revised form 3 April 2011
Accepted 5 April 2011
Available online 12 April 2011

Keywords:
Metals
Mechanical property
Microstructure

ABSTRACT

Interfacial microstructure and properties of Sn–0.7Cu–0.05Ni/Cu solder joints with trace amounts Nd additions have been investigated in this paper. The evolution of interfacial morphology of SCN solder joints with and without the presence of Nd under long-term room ambience was also studied. The greatest improvement to the solderability and tensile strength of SCN-*x*Nd are obtained at 0.05 wt.% Nd. Meanwhile, the morphology and growth of interfacial intermetallic (IMC) layer are greatly improved by adding Nd, and the propensity for IMC spalling from the interface of solder joint is definitely reduced with the presence of rare earth Nd, since the sponge-like structure was completely inhibited in the solder joint containing Nd. In addition, a significant amount of Sn whiskers were present on the surface of $NdSn_3$ phases in the SCN0.15Nd/Cu solder joints, and the reason for this phenomenon has been briefly discussed.

1. Introduction

Under the pressure of environmental regulations dictating the elimination of toxic lead element in microelectronics, large quantities of investigation have been carried out for the substitutes of Sn–Pb solders [1]. Sn–Cu alloy is one of the attractive and cheap lead-free solders, and found wide application in microelectronic industry, which met the needs of low-cost-manufacturing [2]. A wide range of element additions has been added to Sn–Cu solder in order to find the most promising low cost lead-free solders for industrial needs [3]. For instance, many researchers have investigated the effects of minor element additions of Ni to improve the properties of the Sn–Cu solder, as a method of improving its properties and microstructure [4]. The phase stabilizing effect of Ni on Cu_6Sn_5 intermetallic (IMC) in the Sn–0.7 wt.%Cu–0.05 wt.%Ni solder was confirmed through various methods: X-ray diffraction, transmission electron microscopy, differential scanning calorimetry (DSC) [5], and Sn–Cu–Ni ternary phase diagram [6] as well as first principle (*ab intio*) calculation [7]. What is more, rare earth (RE) elements have been called the "vitamin" of metals, and trace amount of RE can greatly influence the properties of solder [8]. Hence they have played a crucial role in the development of novel lead-free solder alloys.

Recently, more and more concerns are focused on the microstructural evolution and reliability of lead-free solder joints. The microstructure of solder joints and the formation and growth behavior of the involved IMC phases during the subsequent thermal treatment have been widely studied in numerous research reports [9]. However, most of these studies mainly foucsed on one element or certain property of solder alloys or joints, but the systematic investigation on the evolution of properties and microstructure of solder joint bearing both Ni and RE elements under room ambience are seldom discussed.

It is widely confirmed that interfacial IMCs initially formed during reactive wetting and then developed during the aging period. The effects of substrates, minor alloying elements, mechanical stress and electromigration as well as thermomigration on the microstructural evolution of interfacial IMCs can be significant under various conditions. The purpose of the current research is to investigate the effects of trace amounts of Nd on properties and interfacial microstructure of Sn–0.7Cu–0.05Ni (SCN) solder joint. Afterwards, the evolution of interfacial microstructures and properties of SCN solder joints with and without the presence of Nd under long-term room ambience condition were studied as well.

2. Experimental details

2.1. Alloy design and preparation

Vacuum-melted ingots of pure Sn, Cu, Ni, Nd (with purity of 99.9 wt.%) were prepared as raw materials. Due to their reactive nature with oxygen, the rare earth element Nd and solder were mixed in a vacuum furnace under N_2 atmosphere. The materials were heated to 950 ± 10 °C for 4 h, and periodically mixed by mechanical

* Corresponding author. Tel.: +86 25 8489 6070; fax: +86 25 5211 2626.
E-mail address: xuesb@nuaa.edu.cn (S.B. Xue).

0925-8388/$ – see front matter © 2011 Elsevier B.V. All rights reserved.
doi:10.1016/j.jallcom.2011.04.037

Table 1
Composition of solder alloys.

Alloys	Cu	Ni	Nd	Pb	Bi	Sb	Sn
Sn–0.7Cu–0.05Ni	0.71	0.05	0	0.012	0.004	0.015	Bal.
Sn–0.7Cu–0.05Ni–0.03Nd	0.69	0.05	0.03	0.012	0.006	0.018	Bal.
Sn–0.7Cu–0.05Ni–0.05Nd	0.71	0.05	0.05	0.012	0.002	0.016	Bal.
Sn–0.7Cu–0.05Ni–0.08Nd	0.70	0.05	0.08	0.013	0.003	0.017	Bal.
Sn–0.7Cu–0.05Ni–1.0Nd	0.71	0.05	1.0	0.014	0.006	0.019	Bal.
Sn–0.7Cu–0.05Ni–1.5Nd	0.70	0.05	1.5	0.012	0.005	0.012	Bal.

stirring using a stainless steel rod, in order to homogenize the liquid solder alloy. Afterwards, all the specimens were air-cooled to room temperature in about 5 min. Part of the as-cast SCN–0.15Nd alloys were re-melted and diluted by the addition of SCN alloy so that six different alloys in as-cast form were prepared. Finally, atomic emission spectroscopy (AES) was used to verify the compositions of as cast solder alloys, and actual chemical compositions of solder alloys is listed in Table 1.

2.2. Solderability test

The solderability tests of SCN-*x*Nd were carried out by means of SAT-5100 Solder Checker (Rhesca Co., Ltd.), with wetting balance method as required by Japan Industry Standard JIS Z 3198-4 (test methods for lead-free solders-Part 4: Methods for Solderability Test by a Wetting Balance Method and A Contact Angle Method), as illustrated in Fig. 1. Entire experiments were performed for 10 s at 255, 275, 295 °C in air atmosphere, where the immersion depth and immersion speed were set as 2 mm and 4 mm/s, respectively. Before the tests, pure Cu foils with sizes of 30 mm × 5 mm × 0.3 mm were ultrasonic cleaned in acetone for 3 min. After cleaned in ethanol, the foils were dried properly and finally coated by flux for testing. The no-clean (NC) flux was used to evaluate the solderability and manufacture the solder joints, as the composition of the flux is determined according to JIS Z 3198 standard. Ten samples were measured regarding the same amount of Nd element under each temperature. The effects of soldering temperature and amount of Nd on the wetting force and wetting time were investigated.

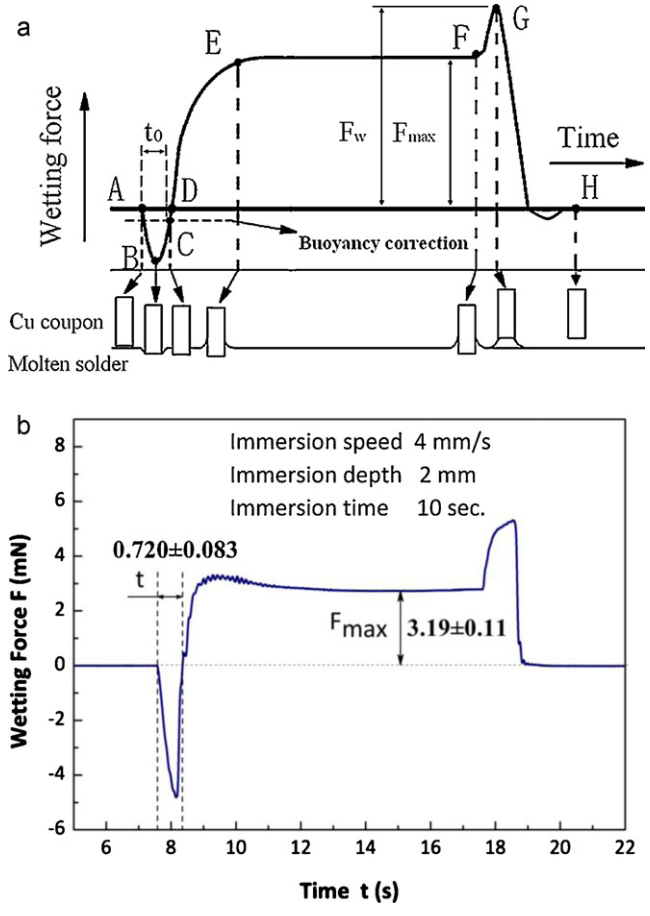

Fig. 1. The wetting balance test: (a) standard wetting curves and (b) wetting curve of SCN0.05Nd solder.

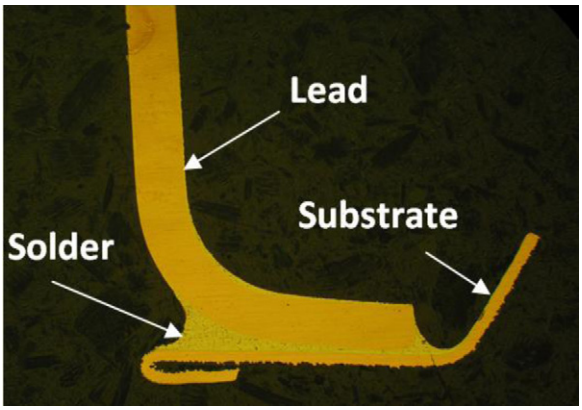

Fig. 2. Magnified image of a solder joint on QFP device.

2.3. Mechanical property test

Aiming to investigate the effects of Nd compositions on mechanical properties of SCN solder joint, Quad Flat Package (QFP32, shown in Fig. 2) were soldered on PCB (Cu/Ni/Au pad) using SCN-*x*Nd with a no-clean flux, and then cleaned with isopropyl alcohol (IPA). After allocating some samples for as soldered joint analysis, others were sent to room ambience. The samples were put into a thermostated container at 25 °C with temperature stability of ±3 °C and aged for 900 h, 1800 h, 2700 h and 3600 h. Subsequently pull tests were carried out according to Japan industry standard JIS Z3198-6 (Test Methods for Lead-free Solders-Part 6: Methods for 45 Degree Pull Test of Solder Joints on QFP Lead) with a STR-1000 joint strength tester. As shown in Fig. 3, the pull tests were conducted at the speed of 2 mm/min. More specifically, ten samples were measured regarding the same amount of Nd element with each room ambience time. After the pull tests, the fracture morphology of solder joints was observed by scan electron microscope (SEM).

2.4. Microstructure observation

Based on the previous solderability and mechanical property test, three kinds of solders (SCN, SCN–0.05 wt.% Nd and SCN–0.15 wt.%Nd) were selected for manufacturing the solder joints. The joints were soldered at 265 °C and heated for about 120 s. All the samples were ultrasonic cleaned in acetone for 5 min. After allocating some samples for analysis in as-soldered state, others were sent to room ambience, with the same method as mentioned in Section 2.3. For interfacial layer observation, specimens were first cross-sectioned perpendicularly to the solder/Cu interface of the solder joints, then packaged in epoxy resin. The specimens were etched with a solution of 5%HNO_3–alcohol for about 2–3 s after grinding and polishing carefully. The microstructure observation was also conducted with SEM.

ImageJ software was used to measure the average thickness of interfacial IMC layer. Firstly, the SEM micrograph was loaded into a computer and the total area of the IMC layer was measured using the software. Secondly the length (thickness) of the IMC was obtained by dividing this area with the SEM micrograph length. Each datum was the average of three images. This method has been used by many other researchers as well.

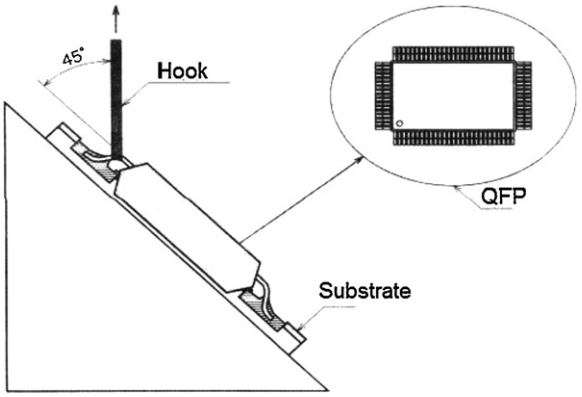

Fig. 3. A schematic of pull test on solder joint in QFP device.

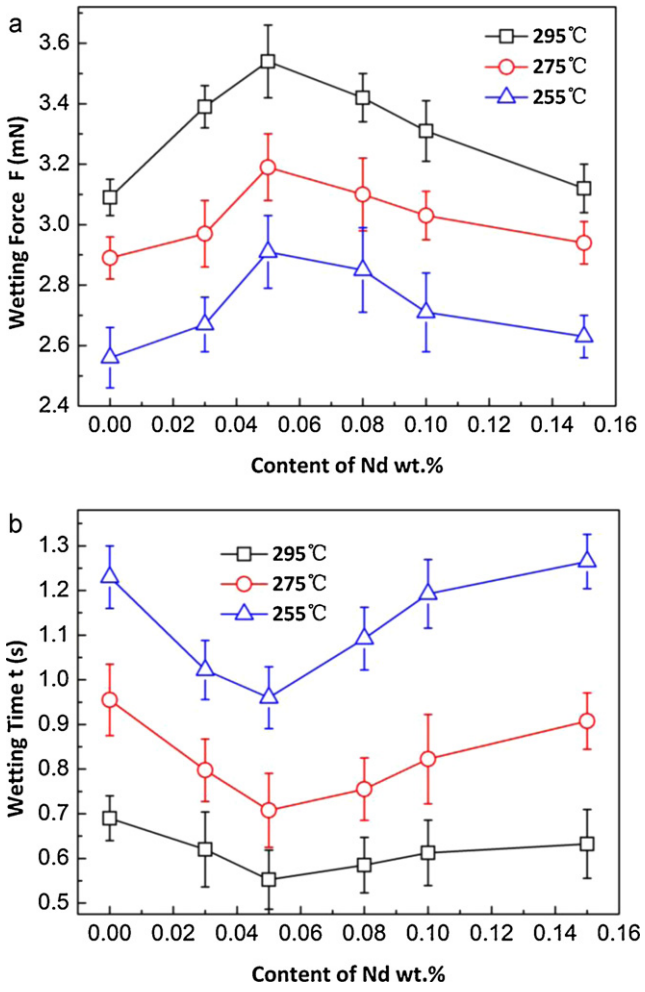

Fig. 4. Solderability of molten solders in air with no-clean flux: (a) wetting force and (b) wetting time of SCN-*x*Nd solder alloys.

3. Results and discussion

3.1. Solderability

Solderability is a measure of the ease with which a solder joint can be made, which is also an essential property to solders for practical application. Therefore, good solderability is considered to be a prime consideration for a new solder alloy, and it is widely accepted that wetting balance method is suitable for measuring the wettability of solder alloys. Solderability is indexed in forms of wetting time and wetting force in wetting balance method, as plotted in Fig. 4. In all solder alloys, the wetting time decreased as the experiment temperature varying from 255 to 295 °C, however, the wetting force ascended with the increase of the temperature. Meanwhile, the wetting time of SCN-*x*Nd solders was all below 1 s at 275 °C, which meets the requirement of automatic soldering technology in electronic industry (i.e. $t_0 < 1$ s), as specified by IPC-J-STD-002C and IPC-J-STD-003B. What's more, as we can see from the line graph, the values of wetting time and wetting force varied over the content of Nd. To be exact, the wetting time of the SCN-*x*Nd solder alloys decreased up to 0.05 wt.% Nd, and increased above 0.05 wt.% Nd. As the content of Nd was 0.05 wt.%, the values of wetting time bottomed at 0.55 s (295 °C), 0.71 s (275 °C) and 0.96 s (255 °C), respectively. It can be clearly seen that the average wetting time of SCN0.05Nd has been reduced by approximately 20% compared to that of the original SCN solder without the presence of Nd. In contrast, the values of wetting force in Fig. 4(a) display a reverse trend over the content of Nd. According to the graph, the values of wetting force increased steadily versus the content of Nd, peaking at 0.05 wt.% Nd. In brief, it is manifested from both of the Fig. 4(a) and (b) that certain amount Nd can significantly improve the solderability of SCN solder. Furthermore, the optimal content of Nd for excellent solderability is 0.05 wt.%, with the range of 0.03–0.08 wt.%.

This improvement obtained by adding trace amount Nd can be attributed to the effects on the interfacial tensions. As an active element, Nd tends to accumulate at the interface of molten solder/air (substrate), which results in a substantial reduction of surface tension of molten solder and enhancement in solderability. However, an excessive amount of Nd addition into the solder alloys can offset the improvement of rare earth Nd, as illustrated in Fig. 4. The main reason is that Nd is prone to be oxidized during soldering, and then the oxidation on surface of solder alloy might increase surface tension and result in the degradation regarding the solderability of SCN0.15Nd solder. Therefore, it is supposed that certain content range of Nd addition is beneficial to the solderability of SCN solder alloy.

3.2. Tensile properties and fracture behavior of solder joint

Pull test was performed to evaluate the effect of Nd on the mechanical reliability of SCN solder joints in both as-soldered state

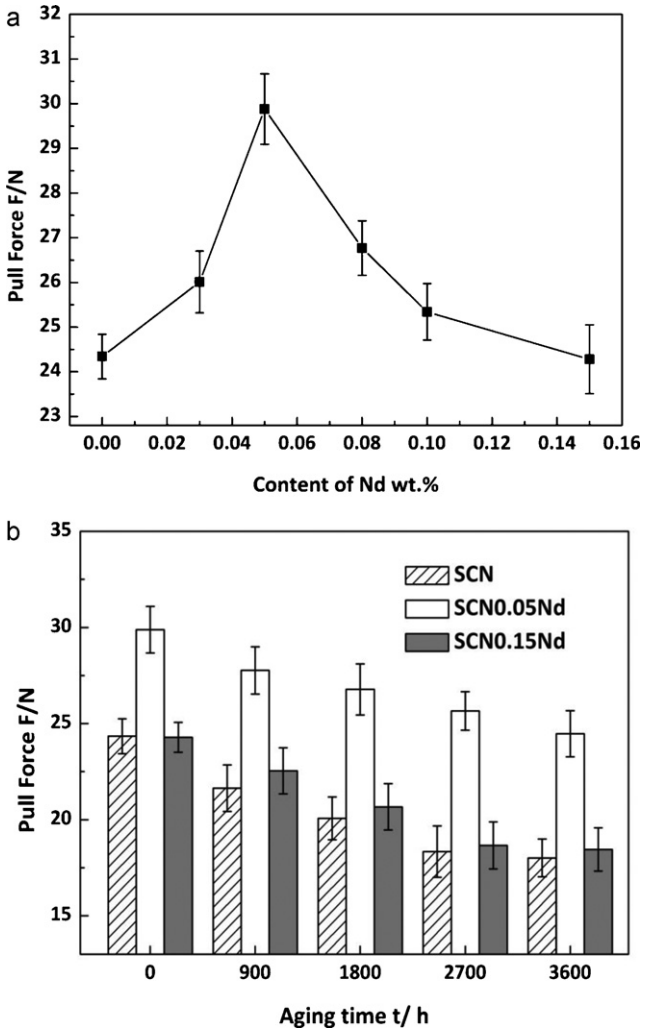

Fig. 5. Pull test results of SCN-*x*Nd solder joints (a) with content in as-soldered state and (b) with time in room ambience condition.

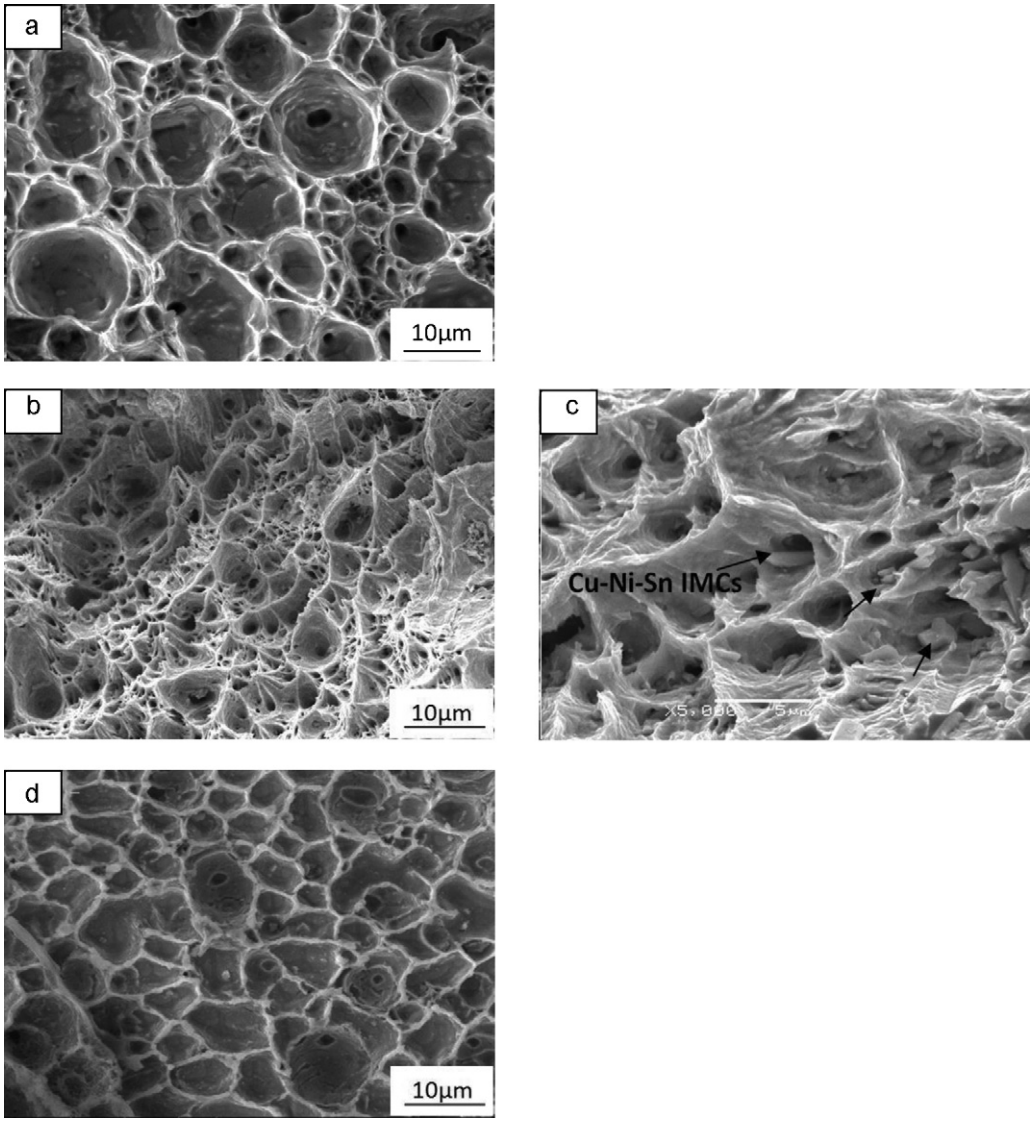

Fig. 6. The fracture surface of solder joint after 3600 h (a) SCN, (b), (c) SCN0.05Nd and (d) SCN0.15Nd.

and room ambience. The test result of as-soldered SCN-*x*Nd solder joints indicated that the pull force of SCN solder joints can be raised by the addition of Nd, and the SCN0.05Nd solder joints yielded the best pull force of 29.88 N compared to other samples. Results also revealed that as the content of Nd increased up to 0.05 wt.%, the pull force values of solder joints continued to increase. However, as the amount of Nd element further increased, the pull force descended. When the content of Nd finally reached 0.15 wt.%, the pull force decreased to 24.28 N, which nearly equals to SCN solder joint.

The bar chart of Pull force–Ambience time regarding SCN, SCN0.05Nd, SCN0.15Nd solder joints is shown in Fig. 5. It can be seen that the pull force of the three sets of solder joints experienced a slight decrease by degrees with increasing time. The pull force decreased to 22.87 N for the SCN0.05Nd joint for 3600 h compared to the as-soldered state, but it was still much larger than that of other two sets of joints. It can be stated that the evolution of pull strength of solder joints at room ambience is greatly affected by the presence of Nd. As the content of Nd was 0.05 wt.%, the solder joints yielded best tensile strength in both as-soldered and room ambience state.

Fig. 6 shows the fracture morphology of SCN, SCN0.05Nd and SCN0.15Nd solder joints after 3600 h aging. Typical dimple fracture surfaces were observed for each solder joint, which indicate that all the solder joints experienced ductile fracture with certain plastic deformation. However, the fracture morphology of the three sets of solder joints displayed somewhat different characteristics. For SCN solder joint, the dimple was relatively large and few IMCs can be observed in the fracture surface, which appeared to be flat and almost lay along the solder/Cu interface. In the case of SCN0.05Nd solder joint, the fracture surface exhibited small dimples appearance and characteristic of large plastic deformation. The sizes of the dimples were much smaller than that of SCN solder joint. It can be clearly seen that the fracture mainly occurred in the bulk solder, with IMC particles existed at the bottom of the dimples. As IMC particles are very hard and brittle, and they are prone to be the stress concentration area, where cracks initiate and then propagate into the solder matrix with approximately 45° with respect to the interface. It can be concluded that small dimples are mainly nucleated by numerous, closely spaced IMC particles, which greatly enhance the strength of the solder joints. SCN0.15Nd solder joints appeared to behave similarly with 0.05Nd solder, but the micro-voids formed during fracture process were much larger in scale than SCN–0.05Nd and fracture surface occurred near the interface of older joint. It can be concluded that the morphology of fracture surface is consistent

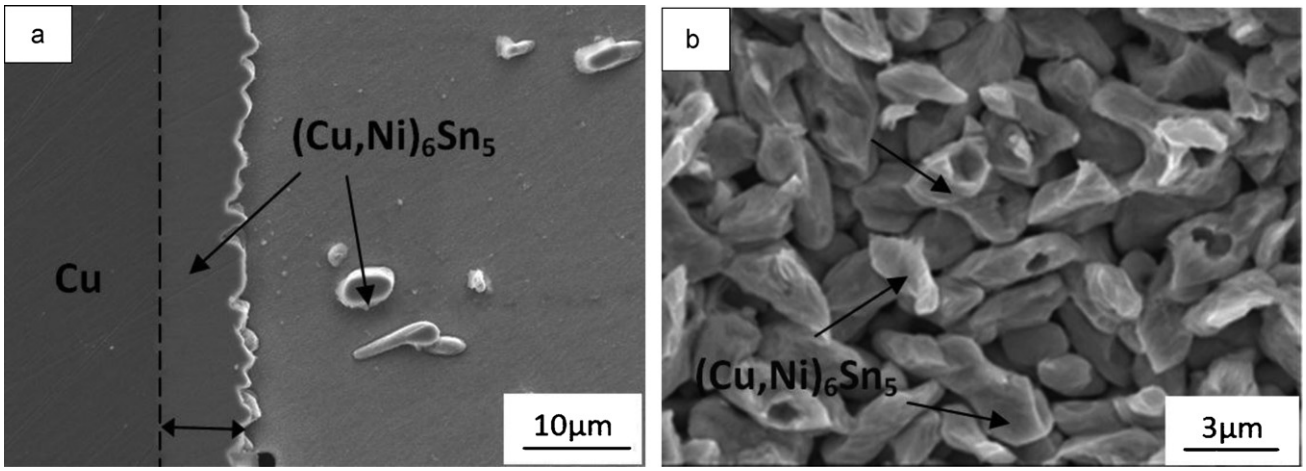

Fig. 7. IMC layer formed between the SCN–0.05 wt.% Nd/Cu as-soldered joints.

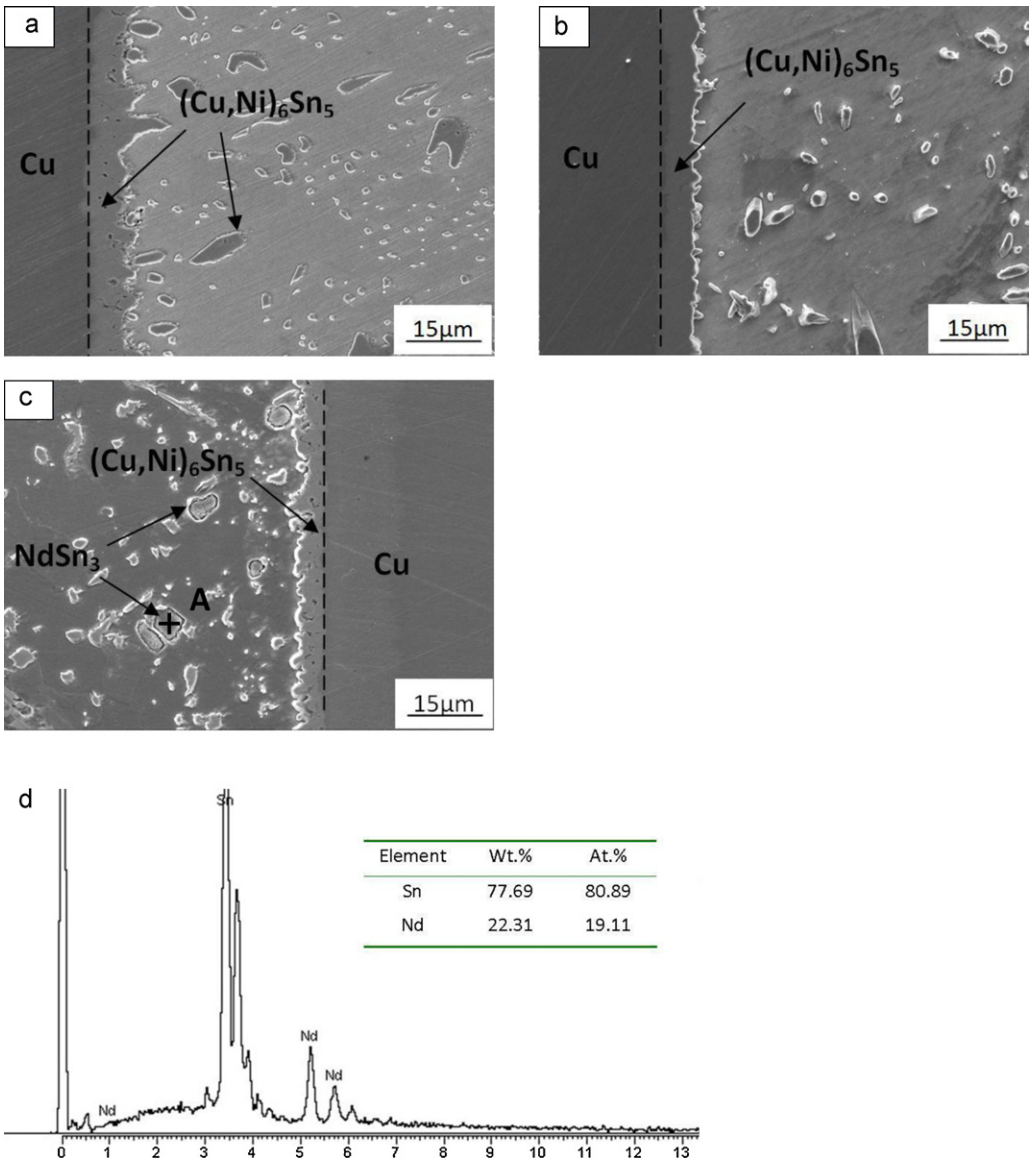

Fig. 8. IMC layer at solder/Cu interface in as-soldered state (a) SCN, (b) SCN0.05Nd and (c) SCN0.15Nd.

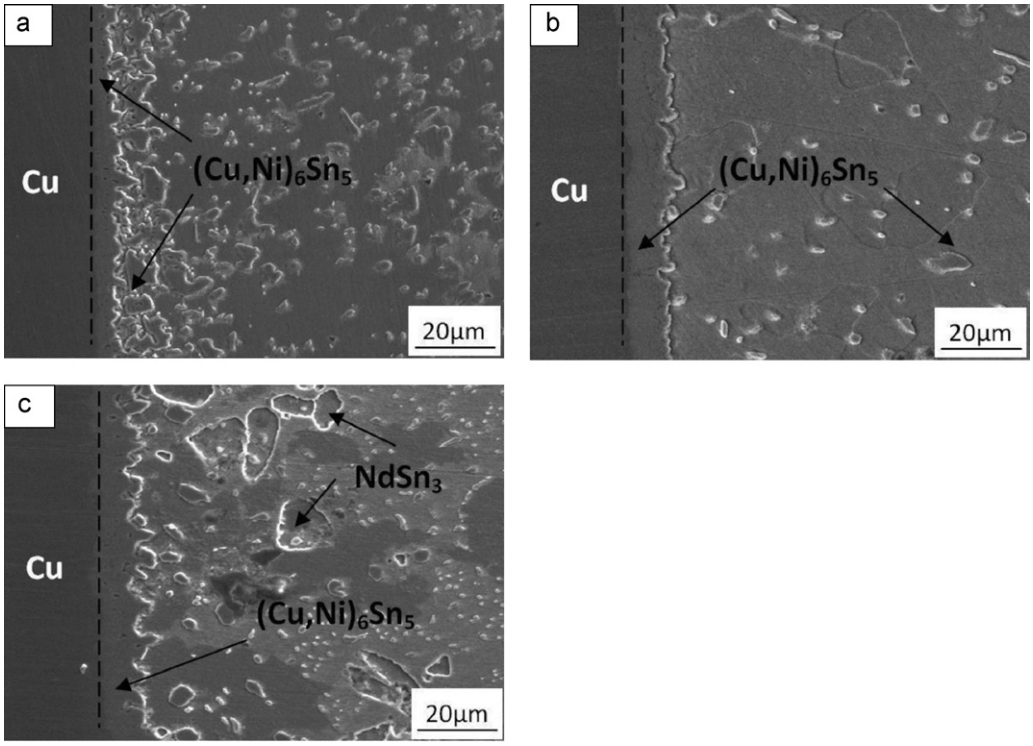

Fig. 9. IMC layer at solder/Cu interface after 1800 h room ambience (a) SCN, (b) SCN0.05Nd and (c) SCN0.15Nd.

with the results of the pull tests. As revealed by Chen et al. [10,11], the position of fracture surface shifting from bulk solder to interface is consistent with the degradation of ultimate tensile strength (UTS). As the SCN0.05Nd solder joint fracture occurred inside the solder, it is considered to have sufficient tensile strength and reliability even if after 3600 h, which is much higher than that of SCN and SCN0.15Nd.

3.3. Morphology of interfacial IMC layer in as-soldered joints

The changes in morphology and thickness of IMC at the interface may greatly influent the mechanical properties of the solder joints. It has been demonstrated that both the thickness of the IMC layers and the interface roughness have an important influence upon the tensile strength and the fracture morphology of the solder joints [8]. During soldering, the solder alloys melt and then react with the substrate to form IMCs at the interface of solder joint. Afterwards, a thin IMC layer is generated at the interface as a reaction product between the solder and substrate. As a consequence, a good metallurgical bond can be achieved. The formation and growth behaviors of IMCs at the interface of joint have been reported extensively in many publications [12–14], where it has been stated that the presence of alloying elements in the solders have strong effects on the properties and growth of IMC layers.

The interfacial structures of SCN-*x*Nd/Cu ($x = 0$, 0.05, 0.15) as-soldered joints are shown in Figs. 7 and 8. The results displayed that IMC layers formed at the interfaces of all solder joints, which ensures the metallurgical bond. The cross-section image of Fig. 7 indicates that the IMC layer is in direct contact with Cu substrate, and the interfacial IMC phases in all cases were confirmed to be $(Cu,Ni)_6Sn_5$ with 7.4–11.2 wt.% Ni by means of EDS analysis. Previously Nogita [5] found that the stabilization of the hexagonal $(Cu,Ni)_6Sn_5$ in Ni-containing solder alloys may prevent volume changes that could contribute to the cracking process in Ni-free solders where the hexagonal-monoclinic transformation occurs at approximately 186 °C. In this study, the morphology of the interfacial IMCs displays recognized differences as the amount of Nd varies. In case of SCN/Cu solder joint, the IMC layer has a rather rough morphology. On the other hand, refer to SCN0.05Nd/Cu solder joints, a relatively flat IMC layer formed at the interface. In comparison, as shown in Fig. 8(c), a large amount of $NdSn_3$ IMCs appeared in the matrix of SCN–0.15Nd solder joint, and it can be referred that the $NdSn_3$ particles greatly contribute to the difference in pull-strength between SCN–0.05Nd and SCN0.15–Nd solder joint. Above all, interfacial IMCs in the solder joint with 0.05 wt.%Nd is relatively flat and slightly thinner than other joints.

In Sn–Cu–Ni/Cu system, the chemical reaction to form interfacial IMCs can be in local equilibrium with the liquid Sn at soldering temperature is [6]:

$$(6-y)\mathrm{Cu} + y\mathrm{Ni} + 5\mathrm{Sn} = (\mathrm{Cu,\ Ni})_6\mathrm{Sn}_5$$

where y is the fraction of Ni atoms in the Cu sub-lattice in Cu_6Sn_5.

The Sn atoms could diffuse into the IMC layer and be the source of $(Cu,Ni)_6Sn_5$ formation. As well known, interfacial reactions forming IMC layers are governed by negative free-energy change. In order to calculate the effect of activities of dissolved Cu and Ni on the stabilities of the IMCs, the following equations for Gibbs energy change of chemical reaction can be derived [12]:

$$\Delta G^{(\mathrm{Cu,Ni})_6\mathrm{Sn}_5} = (1-y)\Delta G_0^{\mathrm{Cu}_6\mathrm{Sn}_5} + y\Delta G_0^{\mathrm{Ni}_6\mathrm{Sn}_5} + RT\ \ln\left[\frac{a_{(\mathrm{Cu,Ni})_6\mathrm{Sn}_5}}{a_{\mathrm{Sn}}^5 a_{\mathrm{Cu}}^{6-y} a_{\mathrm{Ni}}^{y}}\right]$$

From the above equation it can be seen that the left term in the square bracket can be taken as a constant and the Gibbs free energy ΔG is dependent on the activity of Sn at the interface. If the activity of one reactant (Sn, Cu, Ni) decreases, the value in brackets becomes large and thus the driving force for the reaction becomes smaller. Therefore, lowering the activity of Sn should be an effective method to inhibit the growth of the interfacial IMCs of Sn rich solder joint. It has been previously investigated that the driving force for Cu_6Sn_5 IMC formation is reduced by adding a small amount of rare earth, since rare earth elements have a much higher affinity to Sn. The

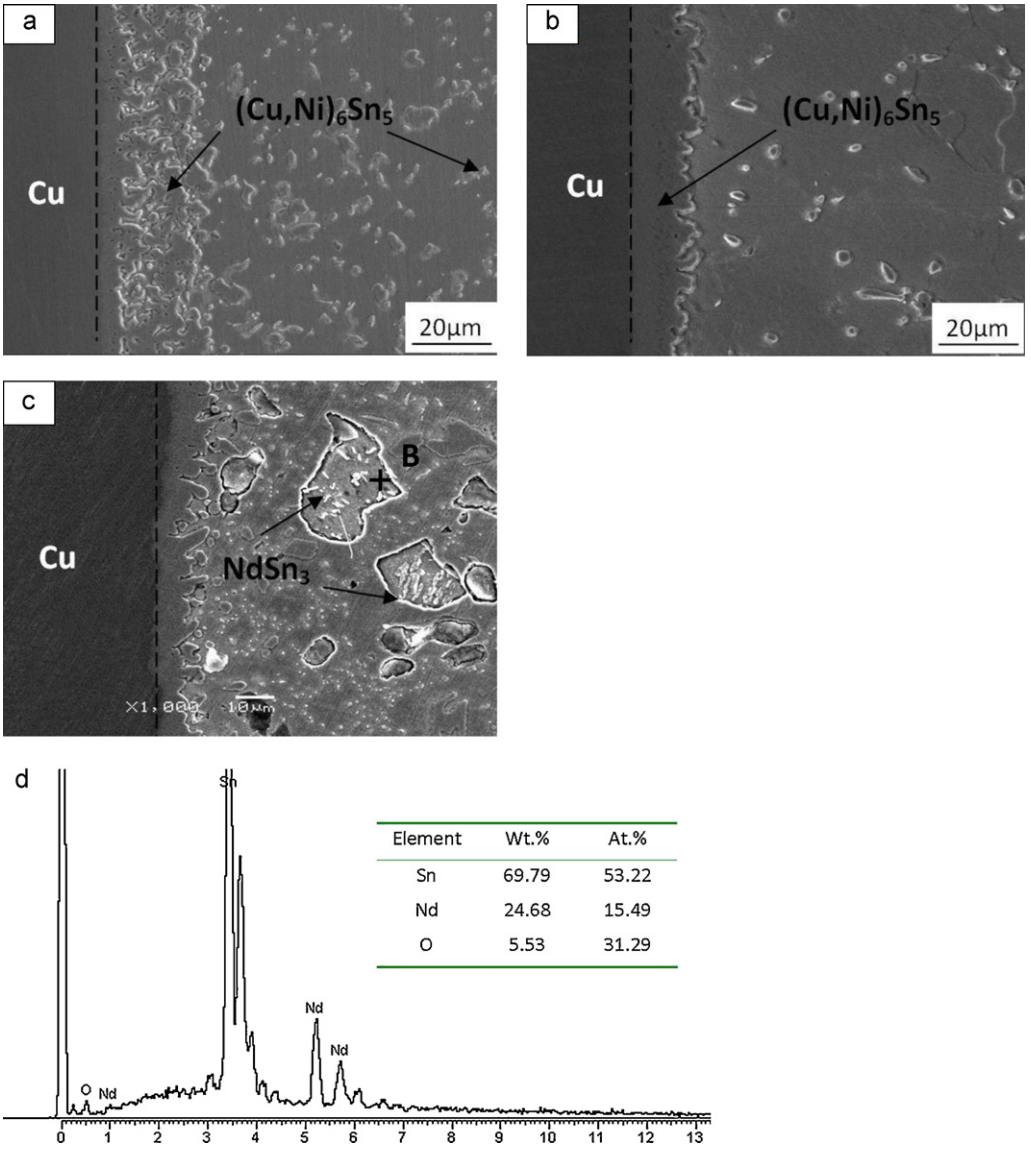

Fig. 10. IMC layer at solder/Cu interface after 3600 h room ambience (a) SCN, (b) SCN0.05Nd and (c) SCN0.15Nd.

electronegativity difference between Nd and Sn is relatively large, in comparison with that of Nd/Cu and Nd/Ni [15]. Therefore the strong interaction between Sn and Nd eventually get the activity of Sn decreased. Above all, it can be summarized that trace amount of Nd can inhabit the growth of interfacial $(Cu,Ni)_6Sn_5$ IMC during soldering.

3.4. Microstructure evolution of interfacial IMCs at room ambience

It is well known that atomic diffusion between the substrate and solder continues in the solid-state reaction period after soldering process. In this study during the subsequent period of room ambience, more notable difference between the Nd containing and Nd-free SCN solder joint has been observed. As the interfacial morphology was observed through SEM, it was found that the IMCs at the SCN-*x*Nd ($x = 0, 0.05, 0.15$)/Cu interface had the morphology changed with the ambient time, as shown in Figs. 9 and 10.

IMCs existed at the interface of the solder joints are confirmed to remain $(Cu,Ni)_6Sn_5$ by EDS analysis. The measured average IMC thickness of the three sets of solder/Cu joint as a function of aging time is summarized in Table 2. It is evident that the IMC thickness show quite different trends for the Nd containing and Nd-free SCN solder joints. It is obvious that the growth rate of IMCs in SCN solder is much faster than that of other two solders bearing Nd. After 1800 h, the thickness of IMC layers in SCN, SCN–0.05Nd and SCN–0.15Nd solder joint has reached about 17.42, 11.19 and 10.88 μm, respectively. Meanwhile, the growth rate of IMC layer in SCN–0.05Nd solder joints was very close to that of 0.15Nd solder joints during the whole aging period. After the 3600 h, the IMC thickness of SCN, SCN0.05Nd and SCN–0.15Nd grew to 26.8, 14.69 and 15.37 μm, respectively. At that time the thickness of the IMC layer of SCN solders bearing Nd is much thinner than SCN solder. In other words, the growth of $(Cu,Ni)_6Sn_5$ IMC was greatly reduced by adding Nd. In addition, although the growth behavior of SCN0.15Nd displayed little difference compared to SCN–0.05Nd, however, large

Table 2
Average IMC thickness at the interface with various ambient time.

Time	0 h	900 h	1800 h	2700 h	3600 h
SCN (μm)	10.45	14.17	17.42	22.34	26.8
SCN0.05Nd (μm)	7.10	8.56	11.19	12.54	14.69
SCN0.15Nd (μm)	7.68	8.33	10.88	12.22	15.37

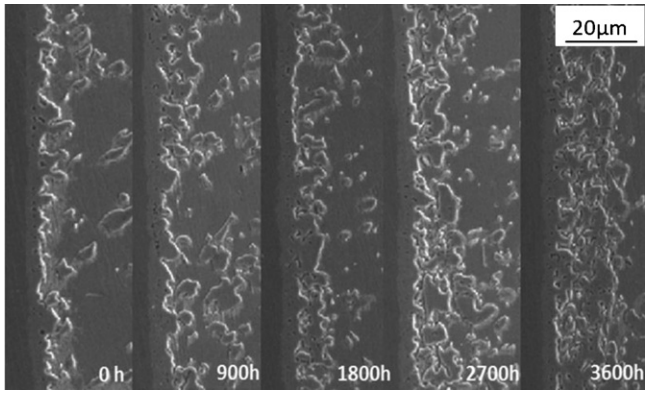

Fig. 11. Spalling behavior of the interfacial $(Cu,Ni)_6Sn_5$ layer in SCN solder joint at room ambience.

amount of $NdSn_3$ IMCs existed in the matrix of SCN–0.15Nd solder joint during the whole process, as shown in Figs. 9 and 10. During the room ambience period, the IMC thickness of SCN0.05Nd has doubled but the interfacial morphology remained evidently flat. In this case the residual stress concentration caused by rough interface can be avoided to some extent, due to the magnitude and complexity of stress distribution can be reduced due to the relatively thin and flat interfacial IMC layer. Another main feature of the interface IMC layer is that there was only a single $(Cu,Ni)_6Sn_5$ layer observed in all the stages, and Cu_3Sn layer was not found within the resolution of the SEM image.

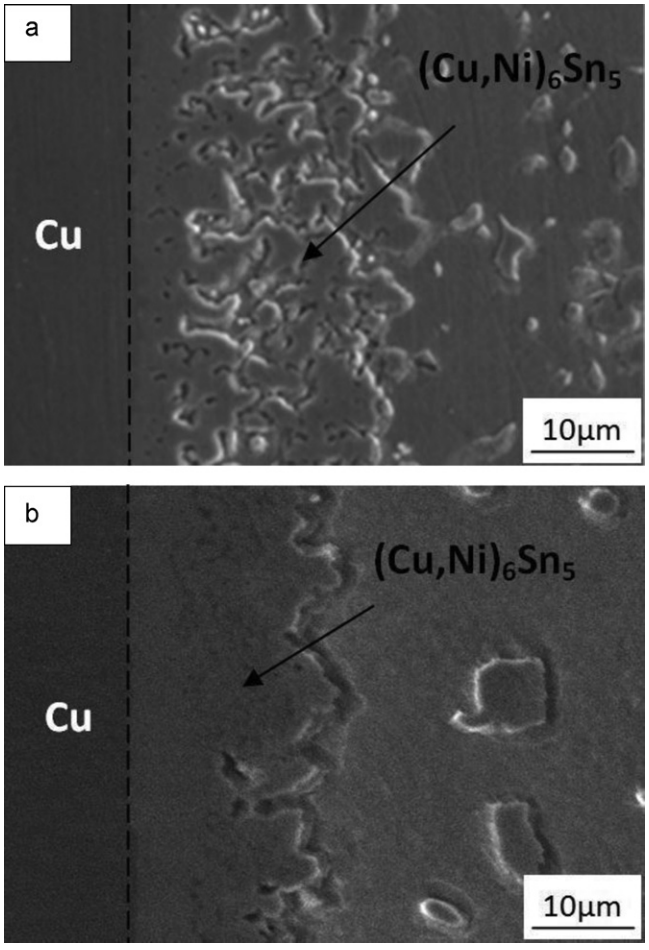

Fig. 12. Difference in the morphology of interfacial IMC layer between (a) SCN/Cu solder joint and (b) SCN0.05Nd solder joint after 3600 h.

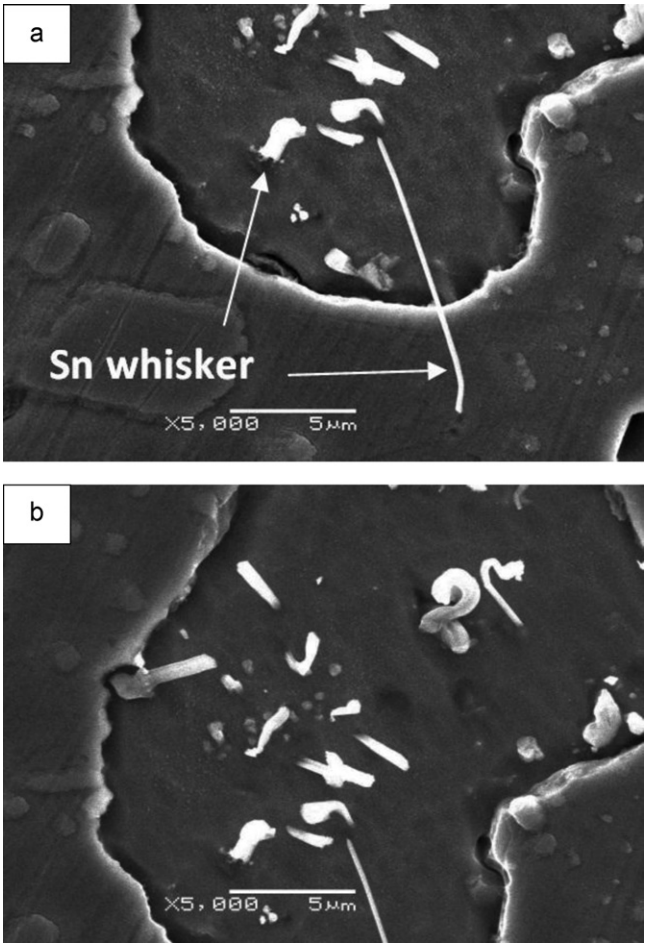

Fig. 13. Hillock and needle-like Sn whiskers grew from the surface of large Sn–Nd phase.

As the atom radius of Nd (0.264 nm) is much larger than the radius of the Sn atom (0.172 nm), the solubility of Nd in β-Sn Phase is rather low, and Nd does not exhibit marked solubility in Cu–Sn–Ni IMCs as well, hence it does not usually participate itself in the solid-state reaction but change the activities of Sn. The presence of Nd dramatically decreases the activity of Sn in the solder and thus reduces the driving force for the diffusion of Sn through the IMC layer, which is called an indirect way to influence the growth of IMC as mentioned above. In summary, the interfacial Cu–Sn–Ni IMC growth at room ambience can be effectively reduced by the addition of Nd into SCN solder.

3.5. Inhibiting effect of Nd on the spalling behavior of interfacial IMC layer

In SCN solder joint, it is noticed that the IMC layer cracked and detached from the interface during exposure to ambient room air. It is called the massive spalling behavior of IMCs by many researchers [16,17], and here spalling refers to the detachment of the IMC compounds at the interface. Fig. 11 shows the whole process of spalling behavior of interfacial IMC layer in the case of SCN/Cu solder joint. At the early stage, no obvious spalling was observed in the as-soldered state. However, after 900 h at room ambience, the thickness of IMC layer is increased to 14.17 μm, and the cracking and spalling of the interfacial IMC layer occurred. More Cu–Ni–Sn IMCs spalled off the interface with the time increased. Another distinguished characteristic of the spalling is the disintegration phenomenon which occurred after 2700 h. Although the

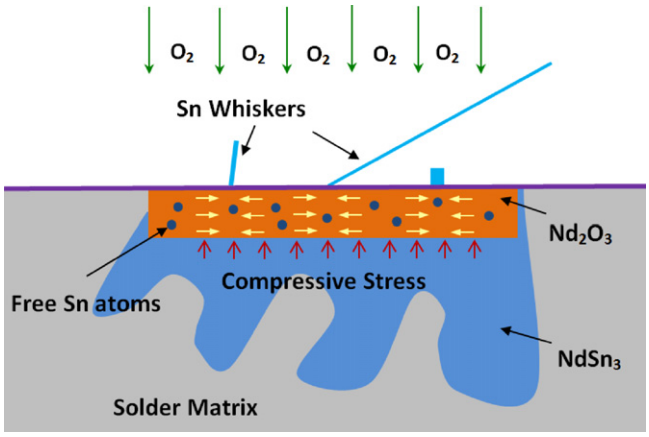

Fig. 14. A schematic of whisker growth driving by an oxidation reaction between the Sn–Nd compound and oxygen in air.

IMCs has detached from the interfacial layer, the spalling IMCs adjacent to the interfacial layer continued to coarsen steadily, and discontinuous $(Cu,Ni)_6Sn_5$ particles were clearly observed after 2700 h room ambience. After 3600 h, a sponge like structure formed near the interface, and there were a large number of discontinued IMC particles inside the layer, which has a great negative influence on the strength of solder joints. In contrast, there was no obvious spalling phenomenon in the case of SCN0.15Nd solder. By the addition of rare earth Nd into the SCN solder, the spalling behavior and the sponge structure at the interface is greatly inhibited. As shown in Fig. 12, the interfacial IMC layer of SCN0.05Nd solder joint is smooth and continuous compared to that of SCN solder joint, which is quite beneficial to the strength of the solder joint. It can be concluded that the propensity for IMC spalling from the interface was definitely reduced with the existence of Nd, which in turn improve the pull strength of solder joint.

3.6. Sn whisker growth on the surface of $NdSn_3$

It has recently been documented that Pb-free solder alloys bearing with trace amounts of rare earth elements show a very strong propensity to grow Sn whiskers [18–22]. In this study, a significant amount of Sn whiskers were present on the surface of $NdSn_3$ phases in the SCN0.15Nd/Cu solder joints after 3600 h room ambience. It can be clearly seen that whiskers grew from the area of Sn–Nd intermetallic in the solder matrix near to the solder/Cu interface. As shown in Fig. 14, a main feature of the Sn whisker growth is that both hillock and needle-like whiskers has grown from the large Sn–Nd phase.

Due to the reactive nature of rare earth element Nd with oxygen, it is prone to severe oxidation even at room ambience. As a result, SCN0.15Nd solder containing Sn–Nd intermetallic phases are prone to grow whiskers. It is demonstrated by the EDS result that $NdSn_3$ intermetallics in the SCN–0.15Nd solder have been oxidized, resulting in a Nd-rich oxide after exposure to room ambience conditions. Gibbs free energies of formation for the Nd_2O_3 phases, SnO and SnO_2 phases are −1720.9, −251.9 and −515.8 kJ/mol, respectively [23]. Therefore, it can be stated that $NdSn_3$ phases are not thermodynamically stable and prone to oxide compared to Sn atoms. Oxidation of the rare earth element Nd in the $NdSn_3$ compound occurs as follows:

$$4NdSn_3 + 3O_2 \rightarrow 2Nd_2O_3 + 12Sn$$

This reaction results in a volume expansion within the original $NdSn_3$ particle. Because the IMC phases are constrained from expansion during oxidation due to the surrounding Sn matrix, the oxidized zone is under a state of compression, which becomes a necessary condition for whisker growth. Meanwhile, according to the reaction equation above, the formation of Nd_2O_3 would release several free tin atoms, which have a high chemical potential [24]. Moreover, these tin atoms can supply a driving force for the rapid Sn whisker growth, which was demonstrated by that many tin nodules existed on the surface of the $NdSn_3$, as displayed in Fig. 13b. The whisker growth may be caused by an oxidation reaction of $NdSn_3$ compound in room ambience: the compressive stress introduced by the phase transformation ultimately result in the formation of whiskers and the fresh Sn atoms reaction move into the root of a whisker to make it grow. In conclusion, the driving force for whisker growth on the surface of large size $NdSn_3$ phases is related to the compressive stress and the free tin atoms which are both generated in the oxidation of $NdSn_3$ intermetallic compounds. Therefore, it further indicates that certain content range of Nd addition is beneficial to properties of SCN solder joint, in order to avoid whisker growth in solder joint.

4. Conclusions

In the present work, the effects of rare earth on the interfacial properties and microstructure of Sn–0.7Cu–0.05Ni (SCN) were investigated. The results are summarized as follows:

1. The solderability of SCN solder on Cu substrates gets improved by adding trace amounts of Nd, and the optimal content of Nd is about 0.05 wt.%, within the range of 0.03–0.08 wt.%. This improvement may be attributed to the accumulation of Nd on the surface of molten solder, which leads to the reduction of the interfacial tensions and improvement of the solderability.
2. The pull strength of SCN solder joint is also enhanced by the addition of Nd. As the content of Nd was 0.05 wt.%, the solder joints yielded best performance in both as-soldered and room ambience state. The morphology of the fracture surfaces of solder joints displayed different characteristics: the fracture of SCN0.05Nd almost occurred in the bulk solder, and that of SCN appeared to be flat and almost lies along the solder/Cu interface. As the SCN0.05Nd solder joint fracture occurred inside the solder, it is considered to have sufficient tensile strength and reliability even if after 3600 h, which is much higher than that of SCN and SCN0.15Nd.
3. The morphology of IMC at the interface of as-soldered joint are greatly influenced by rare earth Nd. The IMC thickness of SCN0.05Nd solder joint was obviously flat and slightly thinner than other joints. Afterwards, the IMC growth at room ambience was also inhibited by proper amount of Nd. Meanwhile, the propensity for IMC spalling from the interface was definitely reduced with the existence of Nd, since the sponge-like structure cannot be observed in the solder joint containing Nd. This phenomenon can be all related to the high activity of Nd atoms, which reduces in the driving force of interfacial reaction and diffusion.
4. A number of $NdSn_3$ IMCs appeared in the matrix of SCN0.15Nd solder joint, and a significant amount of Sn whiskers was present on the surface of $NdSn_3$ phases in the SCN0.15Nd/Cu solder joints after 3600 h. The driving force for the whisker growth on the surface of large size $NdSn_3$ phases can be related to the compressive stress and the free tin atoms which both generated in the oxidation of $NdSn_3$ intermetallic compounds. Therefore the amount of Nd addition should be controlled aiming to avoid Sn whisker growth and secure the reliability of solder joints.

Acknowledgements

The present work was carried out with the supported by Provincial Key Lab of Advanced Welding Technology, Jiangsu University of Science and Technology Foundation (JSAWT-09-02).

References

[1] A. Pietriková, J. Bednarcík, J. Durisin, J. Alloys Compd. 509 (2011) 1550–1553.
[2] X. Li, F. Zhang, F. Zu, X. Lv, Z. Zhao, D. Yang, J. Alloys Compd. 505 (2010) 472–475.
[3] G. Li, Y. Shi, H. Hao, Z. Xia, Y. Lei, F. Guo, J. Alloys Compd. 491 (2010) 382–385.
[4] M.J. Rizvi, C. Bailey, Y.C. Chan, M.N. Islam, H. Lu, J. Alloys Compd. 438 (2007) 122–128.
[5] K. Nogita, Intermetallics 18 (2010) 145–149.
[6] C.H. Lin, S.W. Chen, C.H. Wang, J. Electron. Mater. 31 (2002) 907–915.
[7] U. Schwingenschlogl, C. Di Paola, K. Nogita, C.M. Gourlay, Appl. Phys. Lett. 96 (2010), 061908–061903.
[8] J. Zhou, D. Huang, Y.L. Fang, F. Xue, J. Alloys Compd. 480 (2009) 903–907.
[9] J. Chen, J. Shen, S.Q. Lai, D. Min, X.C. Wang, J. Alloys Compd. 489 (2010) 631–637.
[10] S.W. Chen, S.H. Wu, S.W. Lee, J. Electron. Mater. 32 (2003) 1188–1194.
[11] S.W. Chen, S.W. Lee, M.C. Yip, J. Electron. Mater. 32 (2003) 1284–1289.
[12] T. Laurila, V. Vuorinen, M. Paulasto-Kröckel, Mater. Sci. Eng. R 68 (2010) 1–38.
[13] Y.W. Yen, Y.C. Chiang, C.C. Jao, D.W. Liaw, S.C. Lo, C. Lee, J. Alloys Compd. 509 (2011) 4595–4602.
[14] Y.W. Wang, Y.W. Lin, C.R. Kao, J. Alloys Compd. 493 (2010) 233–239.
[15] L. Gao, S. Xue, L. Zhang, Z. Sheng, G. Zeng, F. Ji, J. Mater. Sci. Mater. El. 21 (2010) 643–648.
[16] Y.C. Lin, T.Y. Shih, S.K. Tien, J.G. Duh, Scr. Mater. 56 (2007) 49–52.
[17] J.W.R. Teo, Y.F. Sun, Acta Mater 56 (2008) 242–249.
[18] M. Liu, A.P. Xian, J. Electron. Mater. 38 (2009) 2353–2361.
[19] M.A. Dudek, N. Chawla, Acta Mater. 57 (2009) 4588–4599.
[20] T. Chuang, J. Alloys Compd. 480 (2009) 974–980.
[21] M. Liu, A.P. Xian, Microelectron. Reliab. 49 (2009) 667–672.
[22] T.H. Chuang, Scr. Mater. 55 (2006) 983–986.
[23] J.G. Speight, Lange's Handbook of Chemistry, 16th ed., McGraw-Hill, New York, 2005.
[24] H. Ye, S. Xue, L. Zhang, Z. Xiao, Y. Hu, Z. Lai, H. Zhu, J. Alloys Compd. 509 (2011) L52–L55.